Human Molecular Genetics, 2008, Vol. 17, No. 5 **656–666**
doi:10.1093/hmg/ddm337
Advance Access published on November 16, 2007

SLC4A11 mutations in Fuchs endothelial corneal dystrophy

Eranga N. Vithana[1,2,*,†] Patricio E. Morgan[3,†], Vedam Ramprasad[5], Donald T.H. Tan[1,2,7], Victor H.K Yong[1], Divya Venkataraman[1], Anandalakshmi Venkatraman[1], Gary H.F. Yam[7], Soumittra Nagasamy[5], Ricky W.K. Law[8], Rama Rajagopal[6], Chi P. Pang[8], Govindsamy Kumaramanickevel[5], Joseph R. Casey[3,4] and Tin Aung[1,2,7]

[1]Singapore Eye Research Institute, 11 Third Hospital Avenue, Singapore 168751, Singapore, [2]Department of Ophthalmology, Yong Loo Lin School of Medicine, National University of Singapore, Singapore 117597, Singapore, [3]Department of Physiology and [4]Department of Biochemistry, University of Alberta, Edmonton, Alberta T6G 2H7, Canada, [5]ONGC Department of Genetics & Molecular biology, Vision Research Foundation and [6]Department of Cornea, Medical Research Foundation, Sankara Nethralaya, 18 College Road, Chennai 600 006, Tamilnadu, India, [7]Singapore National Eye Centre, Singapore 168751, Singapore and [8]Department of Ophthalmology and Visual Sciences, The Chinese University of Hong Kong, Hong Kong Eye Hospital, 147K Argyl Street, Kowloon, Hong Kong

Received July 12, 2007; Revised October 18, 2007; Accepted November 14, 2007

The endothelial (posterior) corneal dystrophies, which result from primary endothelial dysfunction, include Fuchs endothelial corneal dystrophy (FECD), posterior polymorphous corneal dystrophy (PPCD) and congenital hereditary endothelial dystrophy (CHED). Mutations in *SLC4A11* gene have been recently identified in patients with recessive CHED (CHED2). In this study, we show that heterozygous mutations in the *SLC4A11* gene also cause late-onset FECD. Four heterozygous mutations [three missense mutations (E399K, G709E and T754M) and one deletion mutation (c.99-100delTC)] absent in ethnically matched controls were identified in a screen of 89 FECD patients. Missense mutations involved amino acid residues showing high interspecies conservation, indicating that mutations at these sites would be deleterious. Accordingly, immunoblot analysis, biochemical assay of cell surface localization and confocal immunolocalization showed that missense proteins encoded by the mutants were defective in localization to the cell surface. Our data suggests that SLC4A11 haploinsufficiency and gradual accumulation of the aberrant misfolded protein may play a role in FECD pathology and that reduced levels of SLC4A11 influence the long-term viability of the neural crest derived corneal endothelial cells.

INTRODUCTION

Fuchs endothelial corneal dystrophy (FECD; MIM136800) is a relatively frequent, progressive degeneration of the corneal endothelium that leads to a thickened Descemet's membrane, a collagen rich basal lamina secreted by the endothelium. FECD is characterized by the progressive formation of microscopic, refractile, posterior excrescences of Descemet's membrane clinically known as cornea guttata (1). Gradual impairment of endothelial cell function and loss of cells with FECD progression lead to stromal oedema and impaired vision. FECD is usually a sporadic condition but it can also be inherited as an autosomal dominant trait (2,3). Recently two genetic loci mapping on chromosome 13 and 18 were identified through genome wide linkage analyses in large Caucasian kindreds (4,5). A rare subtype of early onset familial FECD is also caused by point mutations in the *COL8A2* gene, which encodes the α2 subtype of collagen VIII, a major component of Descemet's membrane (6,7). With only a single gene identified to date, and only for the rare early onset form of FECD, the disease pathogenesis of the more common late-onset FECD remains poorly understood.

*To whom correspondence should be addressed. Tel: +65 6322 4542; Fax: +65 6322 4599; Email: evithana@yahoo.co.uk, eranga.n.v@seri.com.sg
†The authors wish it to be known that, in their opinion, the first 2 authors should be regarded as joint First Authors.

Other endothelial (posterior) corneal dystrophies, which result from primary endothelial dysfunction include posterior polymorphous corneal dystrophy (PPCD; MIM122000) and congenital hereditary endothelial dystrophy (CHED; MIM121700). This group, all thought to represent defects of neural crest terminal differentiation (8), shares common features of disease such as endothelial metaplasia and the secretion of an abnormal Descemet's membrane (9,10). It is therefore possible that a proportion of them could be clinical manifestations of different mutations of the same gene. Accordingly, mutations in *COL8A2* gene have been identified in both familial FECD as well as in a family with PPCD (6). Therefore the *SLC4A11* gene, recently implicated in recessive CHED (CHED2) (11), also represents a good candidate gene for FECD. A role of *SLC4A11* in FECD is further supported by gene expression profiles of normal and FECD human corneal endothelium by serial analysis of gene expression, which showed *SLC4A11* to be significantly down regulated in the cornea of Fuchs patients (12). The *SLC4A11* gene encodes NaBC1, a member of the SLC4 family of bicarbonate transporters that is reported to function as an electrogenic sodium borate co-transporter (13). Homozygous or compound heterozygous mutations in *SLC4A11* have been identified in individuals with CHED2 (11,14–16) as well as in individuals with Harboyan syndrome (MIM217400), also known as corneal dystrophy with perceptive deafness (CDPD) (17).

In this study we report for the first time the results of mutation analysis of the *SLC4A11* gene in 89 unrelated patients with FECD. We show that heterozygous mutations in *SLC4A11* gene may also play a pathogenic role in the development of the more common late-onset FECD.

RESULTS

SLC4A11 mutation analysis in patients with FECD

A total of 89 subjects with FECD were studied, of whom 64 were of Chinese ethnicity from Singapore and Hong Kong. The affected Chinese probands ranged in age from 52 to 91, with an average age of 65.2 years [standard deviation (SD) 12.7 years]. In the Chinese cohort were 49 females and 15 males. Only eight patients had a family history of FECD; the rest were classified as 'late-onset' sporadic cases. Among the 89 FECD subjects, 25 were from India. The affected Indian probands ranged in age from 28 to 81 years, with an average age of 61.6 years (SD 13.6 years). In the Indian cohort there were eight males and 17 females and only two patients had a family history of FECD; the rest were sporadic cases. The ages of Chinese and Indian patients stated above were their ages when first seen and diagnosed at the corneal clinic.

We identified four heterozygous *SLC4A11* sequence alterations in our study subjects, which could cause disease (Table 1 and Fig. 1A). Clinical and genetic details of all patients with *SLC4A11* mutations are given in Table 2. In a Chinese individual we detected a missense mutation at position c.2126G>A (Gly709Glu). This patient also had a father similarly affected, who is now deceased. We were therefore unable to test for the segregation of this mutation with FECD.

A missense mutation substituting threonine by methionine at codon 754 (Thr754Met) caused by a c.2261C>T mutation was also identified in a sporadic FECD case of Chinese ethnicity. A 2 bp deletion, c.99-100delTC, was identified in yet another sporadic Chinese case. This frameshift mutation alters the amino acids downstream of the deletion and maintains an open reading frame for only 16 codons before the premature termination codon. As this premature termination codon occurs >50 nucleotides upstream of the final splice junction of *SLC4A11*, this mRNA is likely to be a target for non-sense mediated decay (18). In an Indian FECD case a c.1195G>A transition mutation led to the substitution of glutamic acid by lysine at position 399 (Glu399Lys). All three patients were unaware of any family history of disease.

All four sequence variants described above were screened in 354 normal controls, including 144 of Indian and 210 of Chinese ethnicity, with none of the variants identified in the controls. The Chinese control panel consisted of 110 females and 100 males that ranged in age from 60 to 99 years with an average age of 71.8 (SD 6.7). The Indian control panel consisted of 77 females and 67 males that ranged in age from 44 to 91 with an average age of 62.5 (SD 8.2). All missense mutation sites also showed high inter-species conservation indicating that mutations at these sites would be deleterious (Fig. 1B).

In addition, a number of other coding sequence changes were detected amongst both FECD cases and normal controls (Table 1). Among these 15 changes, 10 were silent and five missense. The minor allele frequency of the single nucleotide polymorphisms (SNPs) identified in both cases and controls was not significantly different between the two groups (data not shown). Two of the missense changes (Asn72Thr and Ser565Leu) were identified in two Chinese FECD cases and not in controls. Although one change was identified in a single case each, they were categorized as non-pathogenic as they either involved residues not conserved in homologous sequences or represented conservative substitutions (Supplementary Material, Fig. S1).

Expression of *SLC4A11* mutants in transfected HEK cells

The effect of SLC4A11 mutations, Glu399Lys (E399K), Thr754Met (T754M) and, Gly709Glu (G709E), were assessed in transiently transfected human embryonic kidney 293 cells (HEK293 cells). Coding sequences of complementary DNAs (cDNAs) were N-terminally tagged with haemaglutanin (HA) epitope tags to facilitate immunological detection. Blots were probed at the same time with anti-HA antibody to detect the tagged SLC4A11 protein and with anti-β-actin to normalize for differences in the amount of cellular material loaded in each lane. Immunoblots showed that wild-type (WT) SLC4A11 migrated as two bands of ~80 kDa and of 120 kDa (Fig. 2A). The absence of the 120 and 80 kDa bands in sham-transfected samples indicates the specificity of the signal. Scanning and densitometry quantified the relative amounts of the 120 and 80 kDa forms (Fig. 2B–C).

Analysis of the expression pattern of WT and mutant SLC4A11 revealed dramatic differences (Fig. 2B–C). Expression levels of mutant proteins were lower than WT SLC4A11, although statistical significance was achieved

Table 1. *SLC4A11* coding sequence variants

	Sequence change	Individuals identified	Minor allele frequency (MAF)[b]
Presumed pathogenic variants	c.2126G>A Gly709Glu	FECD, Chinese, familial	–
	c.2261C>T Thr754Met	FECD, Chinese, sporadic	–
	c.99-100delTC S33SfsX18	FECD, Chinese, sporadic	–
	c.1195G>A Glu399Lys	FECD, Indian, sporadic	–
Non-pathogenic variants[a]			
Silent	c.405G>A Ala135Ala	Normal controls+FECD	0.064
	c.481A>C Arg161Arg	Normal controls+FECD	0.368
	c.639G>A Ser213Ser	Normal controls+FECD	0.138
	c.951G>A Thr317Thr	Normal controls+FECD	0.016
	c.1179C>T Phe393Phe	Normal controls+FECD	0.013
	c.1215C>T Ile405Ile	Normal controls+FECD	0.006
	c.1620C>T Leu540Leu	Normal controls+FECD	0.016
	c.1833C>T Cys611Cys	Normal controls	0.006
	c.1938G>A Ala646Ala	FECD	0.016
	c.2499G>A Thr833Thr	Normal controls+FECD	0.146
Missense	c.215A>C Asn72Thr	FECD	0.008
	c.271A>G Met91Val	Normal controls+FECD	0.006
	c.980C>T Ala327Val	Normal controls	0.013
	c.1682C>T Thr561Met	Normal controls	0.006
	c.1694C>T Ser565Leu	FECD	0.008

[a]Correspond to sequence variants identified in the screen of only Chinese individuals.
[b]MAF was calculated by genotyping at least 120 chromosomes of normal controls or FECD cases (for SNPs found only in affected individuals).

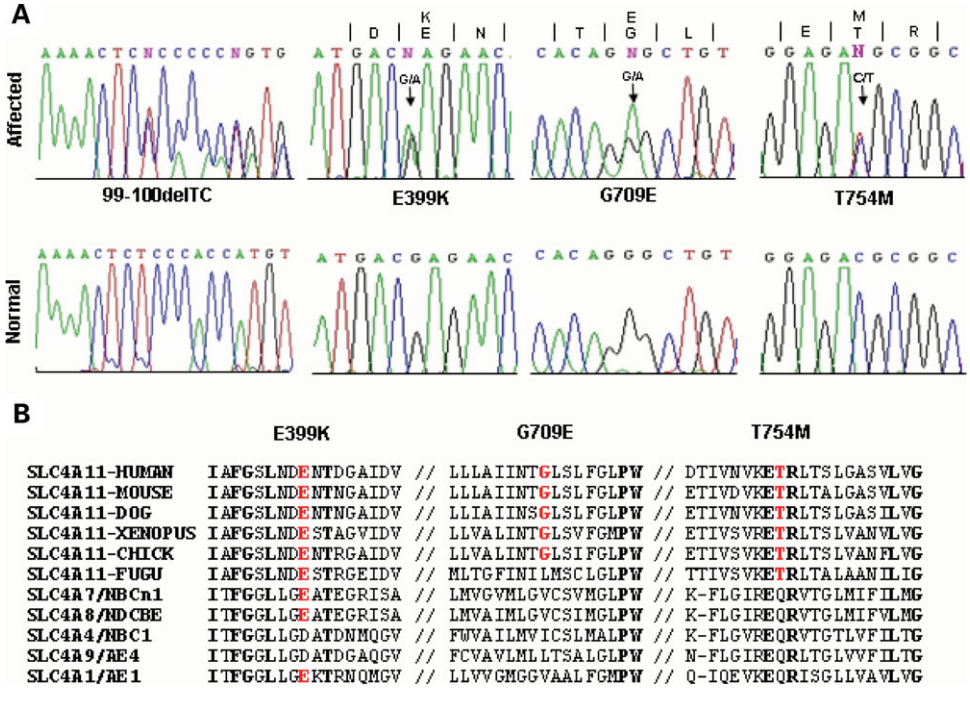

Figure 1. Mutations in *SLC4A11* linked to FECD. (**A**) Sequence electropherograms of the four heterozygous mutations found in *SLC4A11* for FECD. WT sequence from unaffected control individuals is shown in the bottom panel for comparison. (**B**) The conservation of the mutated residues within the SLC4A11 homologs from different species and representative members, NBCn1, NDCBE, NBC1, AE4 and AE1 of the human SLC4 bicarbonate family. Conserved residues are highlighted in bold. The GenBank accession numbers are as follows: human AE1 (P02730), human AE4 (NP_113655.1), human NBCn1 (NP_003606.2), human NDCBE (NP_004849.1), human NBC1 (NP_003750.1), human SLC4A11 (AF336127) and Dog SLC4A11 (XP_542919.1). Mouse SLC4A11 (842 amino acids), *Xenopus* SLC4A11 (858 amino acids), Chick SLC4A11 (836 amino acids) and Fugu SLC4A11 (780 amino acids) are predicted protein sequences from species-specific gene sequences in ENSEMBL genomic database.

only for E399K and G709E (Fig. 2B). The difference was greater in considering the amount of the mature 120 kDa form, where the expression of mutant protein was markedly lower (36 ± 7, 18 ± 4 and 6 ± 3% of WT levels for T754M, E399K and G709K, respectively) than WT SLC4A11 (Fig. 2C). These data were collected with HA-epitope tagged proteins and anti-HA antibody. We have also prepared an antibody directed against a peptide corresponding to the SLC4A11

Table 2. Details of FECD patients with *SLC4A11* mutations

Patient	Ethnicity sex	Mutation	Current age/age at diagnosis	Family history of disease	Ocular history PK	ECD	CCT
1	Chinese (male)	Gly709Glu	61/59	Yes (affected father)	No	730(OD), 1400(OS)	679 OD, 693 OS
2	Chinese (male)	Thr754Met	59/53	No (sporadic)	No	2074(OD), 799(OS)	–
3	Chinese (female)	S33SfsX18	68/60	No (sporadic)	No	2816(OD), 2525(OS)	–
4	Indian (female)	Glu399Lys	59/55	No (sporadic)	PK (OD only)	Cannot measure	570 OD, 554 OS

PK, penetrating keratoplasty; OD, right eye; OS, left eye; ECD, endothelial cell density; CCT, central corneal thickness (μm).

C-terminus. Because the antibody has cross-reactivity towards proteins in untransfected cells, we elected to present data here with the HA-tagged proteins. Nonetheless, untagged SLC4A11 WT and mutants, probed on immunoblots with the anti-SLC4A11 antibody, gave results qualitatively the same as the HA-tagged variants (not shown): 120 and 80 kDa proteins were present and most of WT protein was in the 120 kDa form, while little of the mutant protein reached this mature form. We conclude that the reduced total accumulation of the mutant proteins and the dramatic reduction in maturation to the 120 kDa form are consistent with misfolded proteins that fail to mature and are targeted for degradation.

Cellular localization of SLC4A11 expressed in transfected HEK cells

To assess whether the mutant proteins are defective in their movement to the cell surface, cell surface processing experiments were performed. HEK293 cells transfected with WT and mutant SLC4A11 cDNAs were treated with membrane-impermeant biotinylating reagent (Sulpho-NHS-SS-Biotin, SNSB). After solubilization of the cells, cell lysates were incubated with streptavidin-Sepharose resin to capture biotinylated protein, which represent the protein present at the cell surface. Material remaining in the lysate (unbound, U) therefore represents protein that had an intracellular localization. Additional cell lysate (total fraction, T), not treated with streptavidin-Sepharose, represents the total amount of protein in the sample. Lysates of WT SLC4A11 transfected cells not treated with biotinylating reagent were also incubated with streptavidin-Sepharose resin to act as a control for non-specific binding of protein to resin. Samples of the total and unbound fractions were probed on immunoblots and quantified by densitometry (Fig. 3).

Figure 3B shows that there was a small amount of binding of WT SLC4A11 to streptavidin resin, independent of addition of the SNSB biotinylating reagent, representing the non-specific background of the assay. Streptavidin-bound protein in this assay represents protein accessible to the extracellular medium and thus is at the cell surface. In this context, the fraction of the 80 kDa form of SLC4A11 found at the cell surface is only just above the level of non-specific. In contrast, the fraction of each of the 120 kDa form of SLC4A11 found at the surface was similar for WT and mutant SLC4A11, although there was a slightly higher fraction for WT than for the mutants. We conclude that the 120 kDa form of SLC4A11 is the form found at the cell surface. While Figure 2 shows that little SLC4A11 mutant protein is found as the mature 120 kDa form, Figure 3 indicates that only the 120 kDa form of SLC4A11 is significantly present at the cell surface. Together the data indicate that the level of mutant protein accumulating at the cell surface is only 6–36% of WT levels.

In comparing the SLC4A11 migration on immunoblots we have detected a consistent variation (Figs 2 and 3). In cell surface biotinylation experiments (Fig. 3) we consistently found a larger fraction of WT SLC4A11 present as the upper 120 kDa form than in direct immunoblot experiments. Since we found this even when SNSB reagent was not used (see Fig. 3A WT no SNSB), the difference must result from differences in sample preparation. We attribute the difference to cellular solubilization conditions. In surface biotinylation experiments relatively mild detergent conditions with IPB buffer were used, while the data in Figure 2 were found with cells solubilized directly in sample buffer, containing the strong detergent SDS. The difference thus suggests that SDS solubilizes all of SLC4A11, while IPB buffer is inefficient in solubilizing the lower form of SLC4A11. The failure to solubilize the lower form effectively in IPB is consistent with the presence of 80 kDa form in relatively insoluble protein aggregates.

Confocal microscopic immunolocalization was used as an independent approach to measure SLC4A11 cellular targeting (Fig. 4). In the WT SLC4A11 transfected cells the protein localized predominantly to the plasma membrane. In contrast, SLC4A11 mutants localized with a diffuse distribution in the cytoplasm (Fig. 4). Calsequestrin (CSQ) served as a marker for endoplasmic reticulum (ER) staining. Cells expressing WT SLC4A11 and mutants had the same homogeneous pattern of staining for CSQ. Importantly the merged images indicate significant overlap in staining patterns of CSQ and the SLC4A11 mutants, while co-localization of WT SLC4A11 and CSQ was much more limited. We conclude that the SLC4A11 mutants are retained in the ER, the site of membrane protein biosynthesis, while WT SLC4A11 targets predominantly the plasma membrane.

Glycosylation state of WT and mutant SLC4A11

Glycosylation status of membrane proteins can serve as an indicator of cellular location. Membrane proteins are synthesized in association with the ER membrane, where most membrane proteins are modified by addition of a common 'core' carbohydrate structure at a consensus Asn-X-Ser/Thr site located in an extracellular loop (or ER lumen during biosynthesis). SLC4A11 has two consensus glycosylation sites in the predicted extracellular region, both in extracellular loop 3

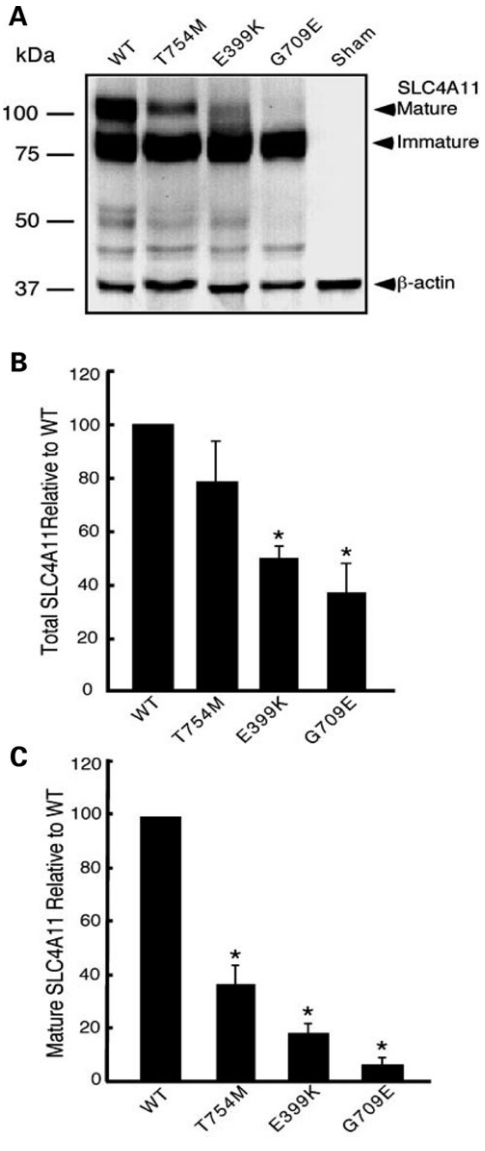

Figure 2. Mutations of SLC4A11 alter the protein's electrophoretic mobility and abundance. HEK293 cells were transfected with cDNA encoding WT or the indicated mutants of HA-tagged SLC4A11. Cells were lysed 48 h after transfection, electrophoresed and probed for the HA tag and for β-actin, as a loading control. (**A**) Immunoblot probed for SLC4A11 (HA-tag) and β-actin. Positions of the 120 kDa (mature) and 80 kDa (immature) forms of SLC4A11 are indicated. Expression of SLC4A11 proteins was quantified by densitometry and normalized to the amount of β-actin. (**B**) Accumulation of SLC4A11 was calculated as: (total amount of 120 kDa+80 kDa SLC4A11, normalized to β-actin) for mutant/(total amount of 120 kDa+80 kDa SLC4A11, normalized to β-actin) for WT × 100%. (**C**) The amount of mature (120 kDa) SLC4A11 was calculated relative to WT as: (amount of 120 kDa form, normalized to β-actin) for mutant/(amount of 120 kDa form, normalized to β-actin) for WT × 100%. Asterisks indicate significant difference ($P < 0.05$), relative to WT SLC4A11, ($n = 5–6$).

(Fig. 5). Core carbohydrate can be removed from proteins by the enzyme, endoglycosidase-H (Endo H). During biosynthesis processing of the core structure in the Golgi apparatus yields a 'complex' carbohydrate that can be cleaved by Peptide N-glycosidase F (PNGase F). Core carbohydrate can also be cleaved by PNGase F.

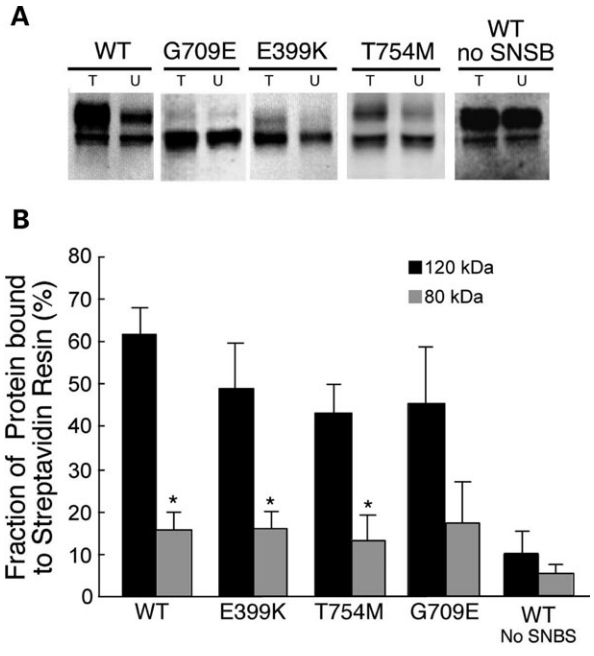

Figure 3. Effect of mutations on SLC4A11 processing to the cell surface. HEK293 cells transfected with SLC4A11 cDNA for the WT or mutant, were labelled with membrane-impermeant SNSB and lysates prepared from the total cellular preparation (T). Biotinylated proteins (accessible at the cell surface) were retained on streptavidin resin and unbiotinylated (intracellular) proteins remained in the unbound lysate (U). (**A**) Immunoblots of total (T) and unbound (U) fractions were probed for HA tag. (**B**) Summary of cell-surface processing of SLC4A11 and mutants. The amount of SLC4A11 on blots was quantified by densitometry. Percentage (%) of SLC4A11 at the cell surface = [(total − unbound)/total) × 100%. Upper band (120 kDa) (black bars) and lower band (80 kDa) (grey bars) were analysed separately. Asterisk indicates significant difference relative to lower band of WT SLC4A11, $P < 0.05$.

To assess the glycosylation state of SLC4A11, lysates were prepared from cells transfected to express N-terminally HA epitope tagged WT and mutant SLC4A11. Lysates were either untreated, or treated with Endo H or PNGase F (Fig. 6). WT SLC4A11 migrated as two bands of 120 and 80 kDa, consistent with previous assessments. PNGase F treatment shifted the protein to a band lower than either the 80 or 120 kDa forms. Treatment with Endo H left the 120 kDa band intact but caused the 80 kDa form to shift to a position coincident with the PNGase F-treated protein. The presence of WT SLC4A11 at the cell surface combined with the shift of the upper band to a position below the 80 kDa form leads to the following interpretation: The 120 kDa form represents complex glycosylation, associated with cellular locations post-ER. The form below 80 kDa represents protein devoid of N-linked glycosylation. The 80 kDa form, shiftable to the position below 80 kDa with Endo H, represents core-glycosylated protein found in the ER. These three bands thus served as markers for mature (complex) glycosylated, core glycosylated and unglycosylated forms of SLC4A11 (Fig. 6). E399K is found predominantly as an Endo H-sensitive (ER) form, but a fraction of the protein was found as a broadly migrating form that was Endo H resistant, but PNGase F-sensitive. This suggests that some of E399K is post-ER, but the position of migration suggests that it is

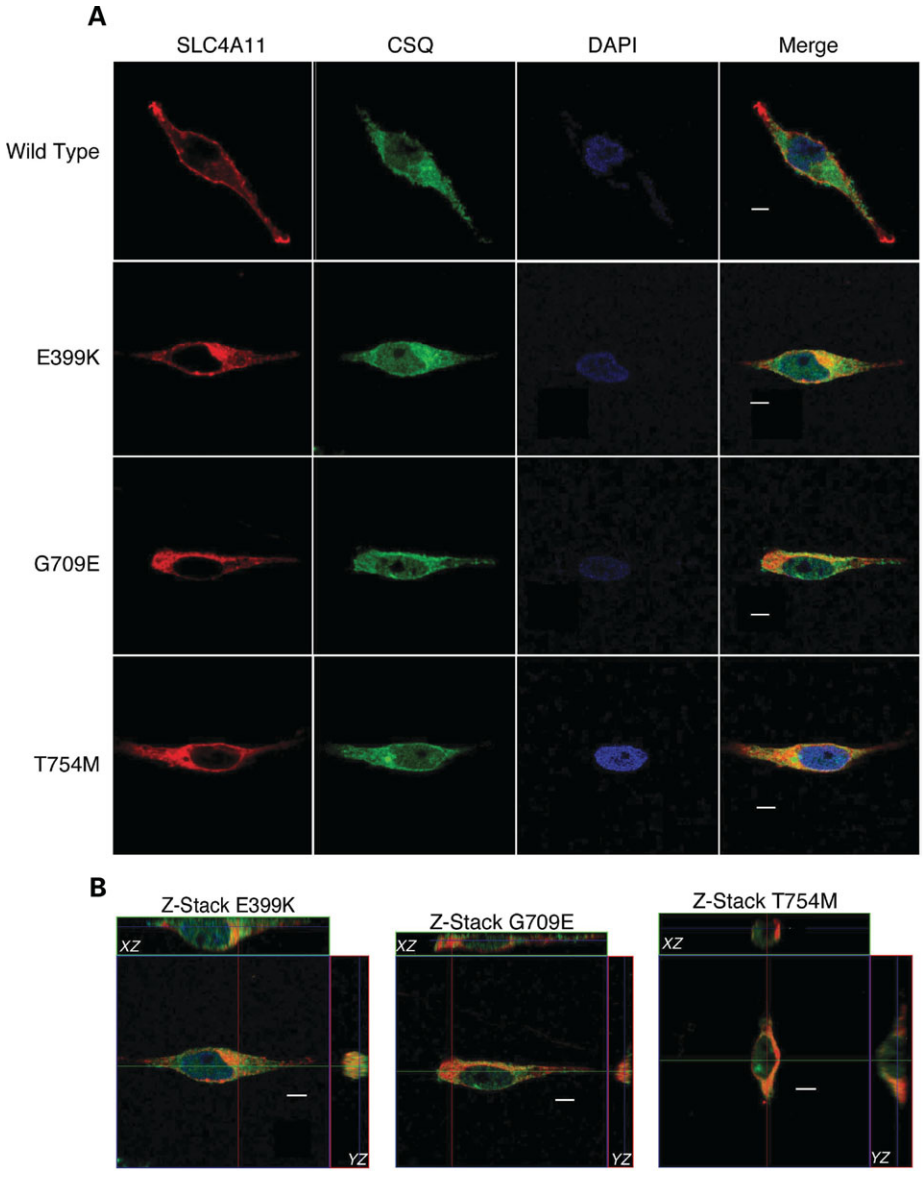

Figure 4. Cellular localization of WT and mutant SLC4A11, expressed in HEK293 cells. HEK293 cells, transiently transfected with cDNA encoding HA-epitope tagged WT and mutant SLC4A11, were stained with mouse anti-HA antibody, followed by Alexa Fluor 594-conjugated IgG secondary antibody (SLC4A11, red). Endogenously expressed CSQ used as an internal control, was stained with rabbit anti-CSQ, followed by Alexa Fluor 488-conjugated IgG (CSQ, green). Nuclei were stained with DAPI (blue). Images were collected with a Zeiss LSM 510 laser-scanning confocal microscope. (**A**) Confocal images of the HEK293 cells transfected with SLC4A11 WT or the mutants G709E, E399K and T754M. (**B**) XZ and YZ cells image reconstruction by stacking confocal images of 0.5 μm thickness. Scale bars = 5 μm.

recognized for glycosylation differently than WT protein in the post-ER environment. In contrast, G709E is found exclusively as an Endo H-sensitive core glycosylated form, consistent with ER-retention. T754M is interesting as it is found as both 80 and 120 kDa forms, which glycosidase treatment revealed to be consistent with ER and post-ER glycosylation forms, respectively.

DISCUSSION

Mutations in *SLC4A11* gene have been recently identified in recessive CHED (CHED2) and its allelic condition Harboyan syndrome or CDPD. In this study, we extend the phenotypes associated with *SLC4A11* gene by showing that heterozygous mutations in the *SLC4A11* gene also cause late-onset FECD. The onset of symptoms for CHED2 and FECD are vastly different, yet the abnormal posterior non-banded zone of the Descemet's membrane points to endothelial dysfunction of both CHED and FECD starting in the late prenatal period. This common disease feature, while underlying the importance of SLC4A11 protein for the correct development and differentiation of the corneal endothelium, may explain how the same gene can be involved in the pathogenesis of both a congenital and a late-onset disease.

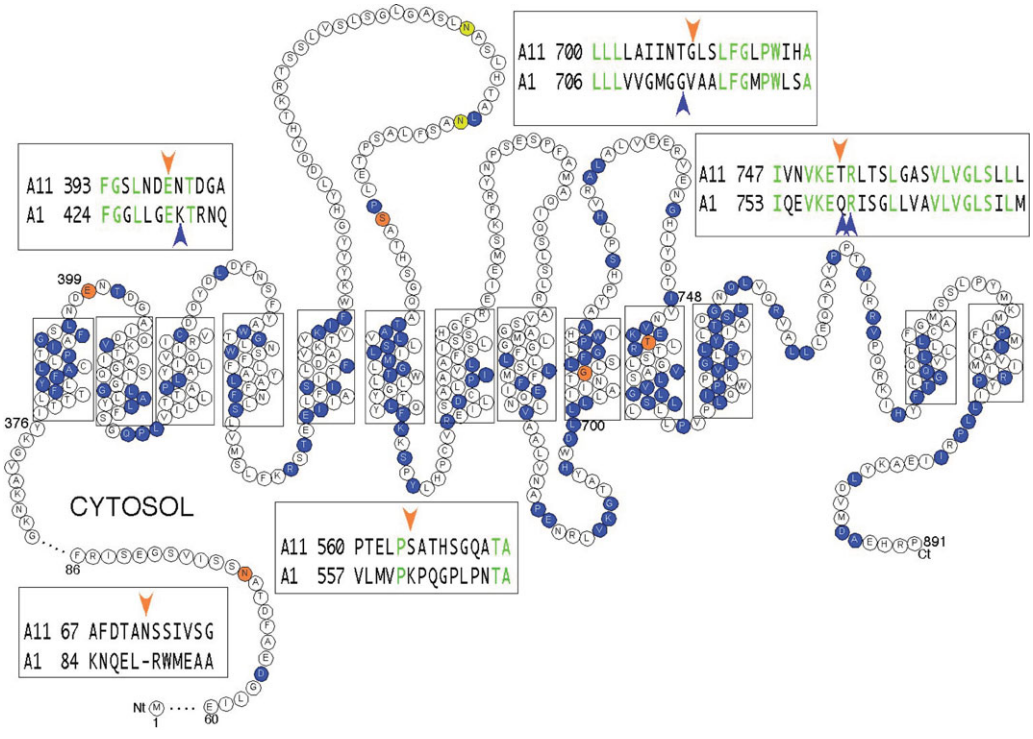

Figure 5. Proposed topology model for human SLC4A11 and location of Fuchs mutations. Topology model was developed on the basis of sequence alignments between human SLC4A1 (AE1) and human SLC4A11 and then applied to a topology model for AE1 (20). Sequence identity between human SLC4A1 and SLC4A11 is indicated by blue filled circles. Consensus N-glycosylation sites are yellow. Locations of Fuchs mutations and the two missense changes (N72T and S565L) deemed non-pathogenic are in orange circles. Inset boxes are alignments of sequences (A11: SLC4A11 and A1: SLC4A1) surrounding the Fuchs mutations. In these boxes sequence identity is in green, orange arrows indicate the position of Fuchs mutation and blue indicates SLC4A1 mutations discussed in the text. Numbers indicate amino acid number.

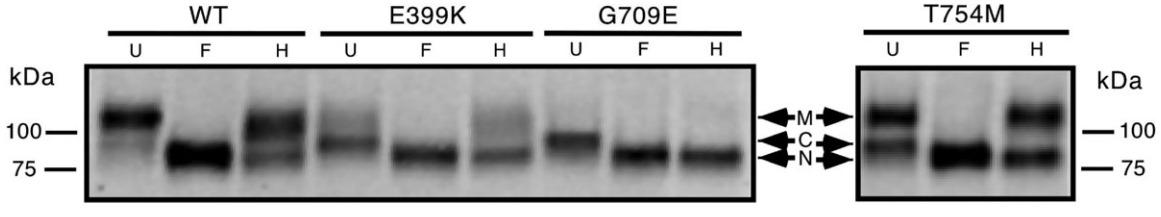

Figure 6. Glycosylation state of SLC4A11 WT and mutants. HEK293 cells were transiently transfected with the cDNA for WT *SLC4A11* and the indicated mutants, each tagged with a HA-epitope tag to facilitate detection. Cell lysate samples corresponding to 10 μg of protein were denatured at 65°C and then treated with either PNGase F (F) or Endo H (H) for 2 h at 37°C. Cell lysate samples (amounts were adjusted to have similar amounts of SLC4A11 in each lane), corresponding to the untreated fraction (U) and fractions treated with Endo H (H) and PNGase F (F) were subjected to SDS–PAGE and corresponding immunoblots were probed for the HA tag with anti-HA antibody. Migration positions of proteins were assigned as mature glycosylated (M), core glycosylated (C) and unglycosylated (N). T754M samples are separated from the other samples because they were treated and analysed concurrently with the other samples, but on a separate gel because the electrophoresis apparatus could not accommodate all the samples on one gel. T754M was electrophoresed along with the same of WT SLC4A11 seen to the left of the figure as a control (data not shown).

We identified four novel heterozygous *SLC4A11* gene mutations that were absent in >350 ethnically matched controls in a screen of 89 FECD patients. The three missense mutations (T754M, G709E and E399K) were shown to have aberrant glycosylation and cellular localization as compared with the WT protein. Our data is consistent with a model in which the identified mutations cause FECD through insufficient SLC4A11 protein levels at the cell surface. Each of the three characterized mutants had in common that little of the protein (6–36% of WT levels) processed to the cell surface. The finding that most of the mutant protein accumulated in the lower molecular mass form, which was poorly soluble in mild detergents, is consistent with ER retention of the mutant protein, leading to targeting for intracellular degradation. The assignment of the 80 kDa form of SLC4A11 as ER-retained was further supported by the sensitivity of this protein to digestion with Endo H.

The primary sequence location of the SLC4A11 mutations associated with FECD provides some insight into their defect. No protein chemical studies of SLC4A11 have yet

been carried out, so there is no experimental evidence for the protein's structure. SLC4A11 has, however, 19–20% amino acid identity with Cl^-/HCO_3^- exchange proteins of the SLC4A family (SLC4A1/AE1, SLC4A2/AE2, SLC4A3/AE3). The membrane domains of human AE1 and SLC4A11 share 24% amino acid identity. There is substantial structural information for the erythrocyte Cl^-/HCO_3^- exchange, AE1 (19–23). Alignment of SLC4A11 with AE1, AE2 and AE3, allowed a topology model for SLC4A11 (Fig. 5), on the basis of a published model for AE1 (20). SLC4A11 appears to have a two-domain structure, with a cytosolic N-terminal domain spanning residues 1–376 and a membrane domain spanning 377–891. Further, this analysis indicates that all of the FECD mutants are in regions conserved across human AE1–AE3 and localize in the membrane domain. E399K is in a small extracellular loop linking the first two transmembrane segments (Fig. 5). Altering the structure in this region might alter the entry of transmembrane segment into the bilayer and could thus affect correct protein folding. G709E and T754M are in regions predicted to be in the plane of the lipid bilayer. These residues could be involved in forming the ion translocation pathway. Since the transmembrane domains are densely packed and involved in protein–protein interactions, mutations here are especially harmful since alteration of the volume of side chains will result in compensatory movement of residues associated with that residue. Consistent with this possibility, G709E and T754M mutations are associated with large changes of side chain volume, 60–111 $Å^3$ (Gly-Glu) and 116–163 $Å^3$ (Thr-Met), respectively. In the case of the G709E, formation of aberrant salt-links is also a possibility associated with introduction of a negatively charged glutamic acid residue.

Diseases affecting other members of the SLC4A family of membrane transporters also support the pathogenicity of SLC4A11 mutations identified in this study. Among SLC4A members, AE1 (band 3/SLC4A1) has the most associated genetic conditions (24,25). The mutations we have identified in SLC4A11 for FECD have parallels to mutations identified in AE1. The G709E mutation lies in predicted transmembrane segment 9 (Fig. 5), where this residue is beside a di-glycine sequence in AE1. In human AE1, the G714R mutation causes hereditary spherocytic anaemia (26). Thus, in adjacent residues of the two proteins, mutating glycine to a charged residue results in a disease allele. The SLC4A11 mutation, T754M, aligns with Q759 of AE1. This part of SLC4A proteins is highly sensitive since mutations at adjacent AE1 residues Q759 and R760 cause distal renal tubular acidosis and hereditary spherocytic anaemia, respectively (25,27). The finding that Q759H mutation in AE1, which aligns with the T754 site in SLC4A11, induces distal renal tubular acidosis further supports the pathogenicity of the SLC4A11 T754M mutation.

Manifestation of the FECD phenotype in individuals with heterozygous *SLC4A11* mutations suggests that FECD will be inherited as a dominant trait. However, we have not been able to demonstrate segregation of the identified mutation with the disease in any of the families; mostly due to the late onset nature of the disease. Family history was only evident for the patient with the G709E mutation, whose father was reportedly affected but deceased, thus precluding any DNA analysis. The other *SLC4A11* mutations, identified in patients with no recorded family history of FECD, may represent *de novo* pathogenic mutations. We are yet unable to determine this for certain or demonstrate co-segregation of these mutations with disease in subsequent generations. This is again due to the non-availability of parental DNA due to death and non-compliance for DNA analysis in some members of the families. This is an ongoing study and we hope to follow up on family members of patients for future clinical and DNA analysis. Identification of heterozygous *SLC4A11* mutations in FECD cases also suggests that heterozygous carrier parents of CHED2 patients should be closely examined for late-onset corneal pathology. This is particularly relevant given that the *in vitro* characteristics displayed in HEK cells by the missense mutant proteins of CHED2 and FECD are very similar. We have not yet detected any clinical pathology in the parents of CHED2 patients characterized in our earlier study (11). This can, however, be attributed to the fact that they are as yet too young to manifest any symptoms. Alternatively, the missense mutations identified in CHED2 patients may be truly recessive and only cause disease in individuals with homozygous mutations.

As seen for SLC4A11 mutations causing recessive CHED and dominant FECD, AE1 mutations cause both dominant and recessive diseases, with the recessive disease forms also being the severest (25). Similar to SLC4A11 mutations causing FECD, many missense mutations in AE1 cause intracellular retention of mutant protein. Erythrocyte instability and distal renal tubular acidosis result from insufficient levels of AE1 at the cell surface. Since AE1 exists only as a dimer, not a monomer (28), mutations that impair plasma membrane trafficking may exert dominant negative effects upon WT protein in heterodimers (24). Given the sequence conservation with AE1, SLC4A11 is also likely dimeric, so heterodimerization of WT and mutant forms of SLC4A11 may also explain dominant inheritance associated with some SLC4A11 mutations. The late onset of the disease and the relative mildness of the phenotype, however, do not support a strong dominant negative effect for *SLC4A11* mutations associated with FECD. There may be a mixture of mechanisms at play, with partial loss of function and gradual accumulation of the aberrant misfolded protein both having a role in FECD pathology.

It is difficult to assess genotype/phenotype correlations for the different *SLC4A11* mutations due to patients being at different stages of disease and incomplete corneal measurements. The central corneal thickness for one of the patients (Patient 2, Table 2) was recorded while having raised intraocular pressure and uveitic glaucoma in both eyes. This misleading measurement was therefore not considered in the phenotype genotype correlation analysis. However, according to age of onset and endothelial cell density, the FECD patient with the c.99-100delTC mutation (S33SfsX18) appears to be the least affected. This mutation results in an early protein truncation and is very likely not to produce any protein product due to degradation of the mRNA by non-sense mediated decay. Therefore, the disease in this case is probably caused by haploinsufficiency. Unfortunately, due to the specificity of *SLC4A11* gene expression or rather the non-expression in lymphocytes, we are unable to determine the stability and fate of this mutant transcript. In future it will

be worthwhile to perform histological and immunohistochemical analyses on the patient corneal buttons and compare the ultra structural details with those without *SLC4A11* mutations. This may provide further insights into molecular mechanisms underlying FECD with *SLC4A11* mutations.

In summary, we have shown that ~5% (4.7%, 95% confidence interval (CI) = 0.98–13.1%) of FECD in the Chinese can be attributed to *SLC4A11* mutations. The sample size studied is too small to allow a precise determination of the *SLC4A11* mutation frequency in the Indian cohort. A similar mutation frequency (4%, 95% CI = 0.1–20.3%) is, however, also suggested in the South Indian FECD cases. The absence of the mutations in age matched controls and the behaviour of the mutant proteins in culture provide convincing evidence that these are indeed disease causing variants and not common polymorphisms. We anticipate that screening of *SLC4A11* gene in FECD patients from other populations will reveal further allelic heterogeneity. The exact role of SLC4A11/NaBC1, reported to be a HCO_3^- independent sodium borate co-transporter (13), in the corneal endothelium is yet unclear, as is the biological relevance of borate to the cornea. Further studies are therefore warranted in gene depleted animal models and in cultured corneal endothelial cells to determine the exact role of NaBC1 in corneal endothelial development and fluid transport, given all indications of its importance to the health of the corneal endothelium.

MATERIALS AND METHODS

Patients and clinical examination

The study protocol had the approval of ethics committees of the participating centres in Singapore, Hong Kong and India and was in compliance with the Declaration of Helsinki. Written informed consent was obtained from all study participants. All patients underwent complete ophthalmic examination, including funduscopy and slit lamp examination and confocal specular microscopy to document corneal guttata. The diagnosis of FECD was based on the presence of greater than 2 mM of confluent central corneal endothelial guttae in each eye or histopathologically confirmed FECD after performing a penetrating keratoplasty or endothelial transplantation. A detailed history was recorded for all subjects, including recording of any family history and duration of onset of symptoms. Peripheral blood samples were collected for DNA analysis. The controls of this study had a normal cornea on ophthalmic examination and no family history of FECD. They were mainly unaffected spouses of patients or were patients undergoing cataract surgery. A total of 354 controls (210 Chinese and 144 Indian) were recruited for this study.

Mutation analysis

Genomic DNA was extracted from leukocytes of the peripheral blood of the patients and exons 1–19 of the *SLC4A11* gene were amplified by polymerase chain reaction (PCR), using primer sequences and PCR conditions described earlier (11). PCR products were purified using GFX PCR clean up columns (Amersham Biosciences AB, Malaysia). Sequence variations were identified by automated bi-directional sequencing using BigDye terminator v3.1 chemistries (Applied Biosystems, Foster City, CA, USA) and an automated DNA sequencer (Model, ABI PRISM 3100, Applied Biosystems, Foster City, CA, USA). Primers for sequence reactions were the same as those for the PCR reaction. Absence of mutations was investigated in either 144 South Indian or 210 Chinese control subjects by direct sequencing of the respective PCR product in which the mutation was identified. Mutation numbering was based on *SLC4A11* cDNA sequence with +1 corresponding to the A of the ATG translation initiation codon in reference sequence NM_032034.1.

Generation of site directed mutants

Cloning of *SLC4A11* cDNA for *in vitro* expression has been described previously (11). Single point mutations identified in FECD patients were introduced into human *SLC4A11* cloned into phCMV2 vector (Gene Therapy Systems, San Diego, CA, USA) using a QuickChange™ site directed mutagenesis kit (Stratagene). The phCMV2 expression vector incorporates an HA epitope tag at the N-terminus of the recombinant protein.

Immunoblot analysis of protein extracts

WT SLC4A11 and mutant variants of SLC4A11 were expressed by transient transfection of HEK293 cells with 1.6 μg of specific cDNA, using the calcium phosphate method (29). Cells were grown at 37°C in an air/CO_2 (19:1) environment in Dulbecco's modified Eagle media, supplemented with 5% (v/v) foetal bovine serum and 5% (v/v) calf serum (Gibco-Invitrogen Corporation, Burlington, ON, Canada). Two days post-transfection, cells were washed with PBS (140 mM NaCl, 3 mM KCl, 6.5 mM Na_2HPO_4, 1.5 mM KH_2PO_4, pH 7.4) and lysates of the whole tissue culture cells were prepared by addition of SDS–PAGE sample buffer [20% (v/v) glycerol, 2% (v/v) 2-mercaptoethanol, 4% (w/v) SDS, 1% (w/v) Bromophenol Blue, 150 mM Tris, pH 6.8]. Prior to analysis, samples were sheared through a 26-gauge needle (BD Biosciences, San Jose, CA, USA) and heated to 65°C for 5 min. Samples were resolved by SDS–PAGE on 7.5% acrylamide gels. Proteins were transferred to PVDF membranes by electrophoresis for 1 h at 100 V at room temperature, in buffer composed of 20% (v/v) methanol, 25 mM Tris and 192 mM glycine. PVDF membranes were blocked by incubation for 1 h in TBST-M buffer [TBST buffer (0.1% (v/v) Tween-20, 137 mM NaCl, 20 mM Tris, pH 7.5], containing 10% (w/v) non-fat dry milk) and then incubated overnight in 10 ml TBST-M [5% (w/v) non-fat dry milk], containing monoclonal mouse anti-HA antibody 16B12 (1:2000) (Covance, Richmond, CA, USA). Blots were incubated for 1 h with 10 ml of TBST-M containing 1:2000 diluted rabbit anti-mouse IgG conjugated to horseradish peroxidase (Amersham Biosciences, NJ, USA). Blots were visualized and quantified, using ECL chemiluminescent reagent (PerkinElmer Life Sciences Inc., MA, USA) and a Kodak Image Station 440CF.

Cell surface processing assays

Assays to assess the degree of cell surface processing and biotinylation of WT and mutant SLC4A11 were performed as described previously (30,31). Briefly, HEK293 cells grown in 100 mm dishes were transiently transfected with WT SLC4A11 and mutant variants of SLC4A11 cDNA as described above. Two days post-transfection cells were washed in phosphate-buffered saline. After washing with borate buffer (154 mM NaCl, 7.2 mM KCl, 1.8 mM $CaCl_2$, 10 mM boric acid, pH 9.0), cells were incubated with 5 ml of borate buffer, containing 0.5 mg/ml SNSB (Pierce, IL, USA) at 4°C for 30 min. After washing three times with cold quenching buffer (192 mM glycine, 25 mM Tris, pH 8.3), cells were solubilized at 4°C in 500 μl IPB buffer (1% Igepal, 5 mM EDTA, 0.15 M NaCl, 0.15% deoxycholate, 10 mM Tris, pH 7.5), supplemented with protease inhibitors (Mini Complete, Roche Molecular Biochemical). Cell lysates were centrifuged for 15 min at 16 000 g, and the supernatant was retained. Half of the supernatant was removed for subsequent SDS–PAGE analysis (total protein). Immobilized streptavidin resin (50 μl of 50% slurry in PBS, containing 2 mM NaN_3, Pierce, IL, USA) was added to the remaining supernatant, which was then incubated overnight at 4°C with gentle agitation. Samples were centrifuged for 2 min at 8000 g, and supernatants were collected and retained for SDS–PAGE analysis (unbound fraction). The resin was washed five times with IPB, and proteins were then eluted from the resin by the addition of 250 μl of SDS–PAGE sample buffer and incubated at 65°C for 5 min. Labelling of the cytosolic protein green fluorescence protein was used as a marker of biotinylation of intracellular proteins (30). The amount of protein was quantified in samples (total protein, unbound fraction, and the fraction eluted from resin) by SDS–PAGE and immunoblotting.

Enzymatic deglycosylation

HEK293 cells were transfected as described above, with HA-tagged SLC4A11 cDNAs. Two days post-transfection, cells were washed with PBS and solubilized by addition of 1 ml of IPB buffer, supplemented with protease inhibitors (Mini Complete, Roche Molecular Biochemical). Bradford assay was used to assess the amount of protein in the cell lysates. Lysate samples (10 μg of protein) were heated 5 min at 65 °C and then incubated with 5 μl (2500 units) of N-glycosidase F (PNGase F) or 3 μl of Endo H (1500 units) (New England Biolabs) for 2 h at 37°C. Reactions were stopped by the addition of 2X SDS–PAGE sample buffer. Samples were electrophoresed on 5% acrylamide Tricine gels (32). Immunoblots were transferred to PVDF membranes and probed with an anti-HA antibody 1:2000 (16B12, Covance Richmond, USA).

Confocal immunolocalization

Cells grown on 22 × 22 mm poly-L-lysine-coated coverslips were transiently transfected as described above. Cells were washed in PBS, and fixed for 20 min in 3.5% (w/v) paraformaldehyde in PBS, containing 1 mM $CaCl_2$, 1 mM $MgCl_2$ (PBSCM). After three washes with PBSCM, cells were incubated for 2 min in PBS, containing 0.1% (v/v) Triton X-100. Slides were blocked for 25 min with PBSG [0.2% (w/v) gelatin in PBS] and incubated with a 1:200 dilution of mouse anti-HA antibody 16B12, and polyclonal 1:100 dilution rabbit anti-CSQ antibody (gift of Dr M. Michalak, Department of Biochemistry, University of Alberta) for 1 h in a humidified chamber at room temperature. After three washes with PBSG, coverslips were incubated for 1 h in a dark humidified chamber with a 1:250 dilutions of Alexa Fluor 594-conjugated chicken anti-mouse IgG, and with Alexa Fluor 488-conjugated chicken anti-rabbit IgG. Coverslips were mounted in Prolong Anti-fade Solution (Molecular Probes, Eugene, OR, USA) and imaged with a Zeiss LSM 510 laser scanning confocal microscope (Germany), mounted on an Axiovert 100M controller with A ×63 (NA1.4) lens. Images of HEK293 cells transiently co-transfected with WT SLC4A11 or mutants of SLC4A11 were taken using the same conditions of illumination and exposure. Images of endogenously expressed CSQ in HEK293 cells were also collected.

Statistical analysis

Values are expressed ± standard error of measurement. Statistical significance was determined using an unpaired *t*-test (Microsoft Excel), with $P < 0.05$ considered significant. CIs for mutation frequencies were calculated using the exact method (33) by assuming binomial distributions of the observed number of patients.

SUPPLEMENTARY MATERIAL

Supplementary Material is available at HMG Online.

ACKNOWLEDGEMENTS

We are grateful to patients for their participation in this study.

Conflict of Interest statement. None declared.

FUNDING

This research is supported by grants from Singapore National Medical Research Council (NMRC-0940/2005), Singapore Eye Research Institute, Indian Council of Medical Research and Vision Research Foundation (VRF Intramural grant 04-2006-P). Canadian Institutes of Health Research supported the research in the J.R.C. laboratory. J.R.C. is a Scientist of the Alberta Heritage Foundation for Medical Research (AHFMR) and P.E.M. is supported by a postdoctoral fellowship from AHFMR.

REFERENCES

1. Adamis, A.P., Filatov, V., Tripathi, B.J. and Tripathi, R.C. (1993) Fuchs' endothelial dystrophy of the cornea. *Surv. Ophthalmol.*, **38**, 149–168.
2. Cross, H.E., Maumenee, A.E. and Cantolino, S.J. (1971) Inheritance of Fuchs' endothelial dystrophy. *Arch. Ophthalmol.*, **85**, 268–272.

3. Rosenblum, P., Stark, W.J., Maumenee, I.H., Hirst, L.W. and Maumenee, A.E. (1980) Hereditary Fuchs' Dystrophy. *Am. J. Ophthalmol.*, **90**, 455–462.
4. Sundin, O.H., Jun, A.S., Broman, K.W., Liu, S.H., Sheehan, S.E., Vito, E.C.L., Stark, W.J. and Gottsch, J.D. (2006) Linkage of late-onset Fuchs corneal dystrophy to a novel locus at 13pTel-13q12.13. *Invest. Ophthalmol. Vis. Sci.*, **47**, 140–145.
5. Sundin, O.H., Broman, K.W., Chang, H.H., Vito, E.C.L., Stark, W.J. and Gottsch, J.D. (2006) A common locus for late-onset Fuchs corneal dystrophy maps to 18q21.2-q21.32. *Invest. Ophthalmol. Vis. Sci.*, **47**, 3919–3926.
6. Biswas, S., Munier, F.L., Yardley, J., Hart-Holden, N., Perveen, R., Cousin, P., Sutphin, J.E., Noble, B., Batterbury, M., Kielty, C. *et al.* (2001) Missense mutations in COL8A2, the gene encoding the alpha2 chain of type VIII collagen, cause two forms of corneal endothelial dystrophy. *Hum. Mol. Genet.*, **10**, 2415–2423.
7. Gottsch, J.D., Sundin, O.H., Liu, S.H., Jun, A.S., Broman, K.W., Stark, W.J., Vito, E.C., Narang, A.K., Thompson, J.M. and Magovern, M. (2005) Inheritance of a novel COL8A2 mutation defines a distinct early-onset subtype of Fuchs corneal dystrophy. *Invest. Ophthalmol. Vis. Sci.*, **46**, 1934–1939.
8. Bahn, C.F., Falls, H.F., Varley, B.S., Meyer, R.F., Edelhauser, H.F. and Bourne, W.M. (1984) Classification of corneal endothelial disorders based on neural crest origin. *Ophthalmology*, **91**, 558–563.
9. McCartney, A.C. and Kirkness, C.M. (1988) Comparison between posterior polymorphous dystrophy and congenital hereditary endothelial dystrophy of the cornea. *Eye*, **2**, 63–70.
10. Levy, S.G., Moss, J., Sawada, H., Dopping-Hepenstal, P.J. and McCartney, A.C. (1996) The composition of wide spaced collagen in normal and diseased Descemet's membrane. *Curr. Eye. Res*, **15**, 45–52.
11. Vithana, E.N., Morgan, P., Sundaresan, P., Ebenezer, N., Tan, D.T.H., Anand, S., Khine, K.O., Venkataraman, D., Yong, V., Salto-Tellez, M. *et al.* (2006) Mutations in Na-borate co-transporter SLC4A11 cause recessive Congenital Hereditary Endothelial Dystrophy, CHED2. *Nat. Genet.*, **38**, 755–757.
12. Gottsch, J.D., Bowers, A.L., Margulies, E.H., Seitzman, G.D., Kim, S.W., Saha, S., Jun, A.S., Stark, W.J. and Liu, S.H. (2003) Serial analysis of gene expression in the corneal endothelium of Fuchs' dystrophy. *Invest. Ophthalmol. Vis. Sci.*, **44**, 594–599.
13. Park, M., Li, Q., Shcheynikov, N., Zeng, W. and Muallem, S. (2004) NaBC1 is a ubiquitous electrogenic Na^+ coupled borate transporter essential for cellular boron homeostasis and cell growth and proliferation. *Mol. Cell.*, **16**, 331–341.
14. Jiao, X., Sultana, A., Garg, P., Ramamurthy, B., Vemuganti, G.K., Gangopadhyay, N., Hejtmancik, J.F. and Kannabiran, C. (2007) Autosomal recessive corneal endothelial dystrophy (CHED2) is associated with mutations in SLC4A11. *J. Med. Genet*, **44**, 64–68.
15. Kumar, A., Bhattacharjee, S., Prakash, D.R. and Sadanand, C.S. (2007) Genetic analysis of two Indian families affected with congenital hereditary endothelial dystrophy: two novel mutations in SLC4A11. *Mol. Vis.*, **13**, 39–46.
16. Ramprasad, V.L., Ebenezer, N.D., Aung, T., Rajagopal, R., Yong, V.H.K., Tuft, S.J., Viswanathan, D., El-Ashry, M.F., Liskova, P., Tan, D.T.H. *et al.* (2007) Novel SLC4A11 mutations in patients with recessive congenital hereditary endothelial dystrophy (CHED2). Mutation in brief #958. Online. *Hum. Mutat.*, **28**, 522–523.
17. Desir, J., Moya, G., Reish, O., Van Regemorter, N., Deconinck, H., David, K.L., Meire, F.M. and Abramowicz, M.J. (2007) Borate transporter SLC4A11 mutations cause both Harboyan syndrome and non-syndromic corneal endothelial dystrophy. *J. Med. Genet.*, **44**, 322–326.
18. Wilusz, C.J., Wormington, M. and Peltz, S.W. (2001) The cap-to-tail guide to mRNA turnover. *Nat. Rev. Mol. Cell. Biol*, **2**, 237–246.
19. Zhu, Q. and Casey, J.R. (2004) The substrate anion selectivity filter in the human erythrocyte Cl-/HCO3- exchange protein, AE1. *J. Biol. Chem.*, **279**, 23565–23573.
20. Zhu, Q., Lee, D.W.K. and Casey, J.R. (2003) Novel topology in C-terminal region of the human plasma membrane anion exchanger, AE1. *J. Biol. Chem.*, **278**, 3112–3120.
21. Tang, X.-B., Kovacs, M., Sterling, D. and Casey, J.R. (1999) Identification of residues lining the translocation pore of human AE1, plasma membrane anion exchange protein. *J. Biol. Chem.*, **274**, 3557–3564.
22. Tang, X.B., Fujinaga, J., Kopito, R. and Casey, J.R. (1998) Topology of the region surrounding Glu681 of human AE1 protein, the erythrocyte anion exchanger. *J. Biol. Chem.*, **273**, 22545–22553.
23. Reithmeier, R.A.F., Chan, S.L. and Popov, M. (1996) Structure of the erythrocyte band 3 anion exchanger. In Konings, W.N., Kaback, H.R. and Lolkema, J.S. (eds), *Transport Processes in Eukaryotic and Prokaryotic Organisms*, Elsevier Science, New York, Vol. **2**, pp. 281–309.
24. Cordat, E. (2006) Unraveling trafficking of the kidney anion exchanger 1 in polarized MDCK epithelial cells. *Biochem. Cell. Biol.*, **84**, 949–959.
25. Alper, S.L. (2006) Molecular physiology of SLC4 anion exchangers. *Exp. Physiol.*, **91**, 153–161.
26. Kanzaki, A., Hayette, S., Morle, L., Inoue, F., Matsuyama, R., Inoue, T., Yawata, A., Wada, H., Vallier, A., Alloisio, N., Yawata, Y. and Delaunay, J. (1997) Total absence of protein 4.2 and partial deficiency of band 3 in hereditary spherocytosis. *Br. J. Haematol.*, **99**, 522–530.
27. Choo, K.E., Nicoli, T.K., Bruce, L.J., Tanner, M.J., Ruiz-Linares, A. and Wrong, O.M. (2006) Recessive distal renal tubular acidosis in Sarawak caused by AE1 mutations. *Pediatr. Nephrol.*, **21**, 212–217.
28. Casey, J.R. and Reithmeier, R.A.F. (1991) Analysis of the oligomeric state of Band 3, the anion transport protein of the human erythrocyte membrane, by size exclusion high performance liquid chromatography: oligomeric stability and origin of heterogeneity. *J. Biol. Chem.*, **266**, 15726–15737.
29. Ruetz, S., Lindsey, A.E., Ward, C.L. and Kopito, R.R. (1993) Functional activation of plasma membrane anion exchangers occurs in a pre-Golgi compartment. *J. Cell Biol.*, **121**, 37–48.
30. Fujinaga, J., Loiselle, F.B. and Casey, J.R. (2003) Transport activity of chimaeric AE2-AE3 chloride/bicarbonate anion exchange proteins. *Biochem. J.*, **371**, 687–696.
31. Sterling, D., Reithmeier, R.A. and Casey, J.R. (2001) A transport metabolon. Functional interaction of carbonic anhydrase II and chloride/bicarbonate exchangers. *J. Biol. Chem.*, **276**, 47886–47894.
32. Schagger, H. and von Jagow, G. (1987) Tricine-sodium dodecyl sulfate-polyacrylamide gel electrophoresis for the separation of proteins in the range from 1 to 100 kDa. *Anal. Biochem.*, **166**, 368–379.
33. Clopper, C.J. and Pearson, E. (1934) The use of confidence intervals for fiducial limits illustrated in the case of the binomial. *Biometrika*, **26**, 404–413.